The 2014 World Congress on
Advances in Civil, Environmental, and Materials Research (ACEM14)
Busan, Korea, August 24-28, 2014

Effect of aerodynamic damping related to the phenomenon of wake galloping of two circular cylinders

*Haeyoung Kim[1)], Tetsuya Kitagawa[2)]

[1)]*Department of Civil Engineering, Yokohama National University, Yokohama, Kanagawa, Japan*
[2)]*Department of Humanity and Environment, Hosei University, Tokyo, Japan*
[1)]*kimhy@ynu.ac.jp*

ABSTRACT

To clarify the mechanism of the wake galloping of two circular cylinders, the aerodynamic damping effect on downstream cylinder is investigated by three-dimensional fluid dynamics computations. Aerodynamic instability caused by the negative aerodynamic damping results in the structure vibrating continuously or even more large. The balance between the structural damping and the aerodynamic damping is calculated in cases of the initial displacement of downstream cylinder, y_s = 0, 0.2, 0.25 and 0.5 at which the fluid speed is 6.6m/s. In the most cases of this research, the structural damping and aerodynamic damping are balanced so that the amplitudes of response displacement on downstream cylinder are stabilized.

1. INTRODUCTION

When the cylinder structure does not exist singularly but in pair or in a group, the flow behavior becomes more complex and difficult to estimate. Especially, the wake galloping is well known to occur aerodynamic instability caused by the negative aerodynamic damping which brought the structure vibrating continuously or even more large. In this research, the aerodynamic damping effect is focused to understand the mechanism of wake galloping. Numerical flow simulations were performed by employing the large eddy simulation with the Smagorinsky subgrid-scale model. To simulate the moving boundary, ALE description is used. Flow around two circular cylinders of equal diameter has been simulated at subcritical Reynolds number (22000), where the upstream cylinder is fixed and the downstream one has a single degree of freedom transverse to the approach flow direction, as shown in Fig.1. The center-to-center spacing of the cylinders is twice the cylinder diameter, and the approach flow speed and the initial displacement of the downstream cylinder are varied. The non-dimensional displacement is defined as the displacement divided by the cylinder diameter. In case of initial displacement, y_S= 0, 0.2, 0.25 and 0.5, the fluid velocity is set to 6.6m/s, respectively.

[1)] Research Associate
[2)] Professor

More details on the numerical simulation methods can be found in the paper by Kim and Kitagawa (2008, 2011). Numerous studies have been carried out to investigate flows around bodies in various arrangements and the fluid dynamic forces acting on them, because of their importance in many engineering applications in the design of structures and in prevention of accidents and disasters. : e.g. Bearman & Wadcock (1973), King & Johns (1976), Bokaian et al. (1984), Igarashi (1984), Williamson (1985), Sun et al. (1992), Zhang & Melbourne (1992), and Gu & Sun (1984). And the numerical investigations on flows around two circular cylinders have been performed for a recent decade. An analytical approach to wake interference effects on circular cylindrical structures was investigated by Rupert. et al.(2006). Many researchers have focused on the flow pattern and phenomenon itself. The mechanism of wake galloping is not clarified yet. Therefore, in this study, the phenomenon of wake galloping is discussed with the aerodynamic damping effect.

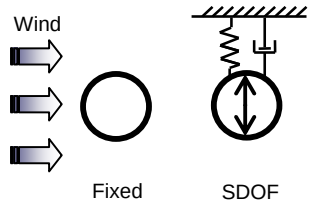

Fig.1. Geometry setting of two circular cylinders in tandem arrangement

2. ANALYTICAL FORMULATION

The non-dimensional equation of motion for the downstream cylinder is

$$m\frac{\partial^2 y}{\partial t^2} + c\frac{\partial y}{\partial t} + ky = \frac{1}{2}C_L \tag{1}$$

The non-dimensional displacement of the downstream cylinder, *y*, can be represented as following cosine function

$$y = y_0 \cos\left(2\pi f_0 t\right) \tag{2}$$

where y_0 is the non-dimensional amplitude and f_0 is the non-dimensional natural frequency. The differential form of *y* for *t* is written as

$$\frac{\partial y}{\partial t} = -y_0 \cdot 2\pi f_0 \cdot \sin\left(2\pi f_0 t\right) \tag{3}$$

On the other hand, we denote the f_0 component of C_L as C_{L0}, and the equation of motion for C_{L0} is

$$m\frac{\partial^2 y}{\partial t^2}+c\frac{\partial y}{\partial t}+ky=\frac{1}{2}C_{L0} \tag{4}$$

By the Fourier transform, C_{L0} can be decomposed such as

$$C_{L0}=\{C_R\cos\ (2\pi f_0 t)-C_I\sin\ (2\pi f_0 t)\} \tag{5}$$

where, C_R is the lift coefficient of the same phase with the response displacement and C_I is the lift coefficient of the same phase with the velocity. These are represented as

$$C_R=\int C_L\cos(2\pi f_0 t)dt \quad , \quad C_I=\int C_L\sin(2\pi f_0 t)dt \tag{6), (7}$$

respectively. By substituting Ep. (6) and (7) into Eq. (4), it can be rewritten as

$$m\frac{\partial^2 y}{\partial t^2}+\left\{-2\pi f_0 y_0 c+\frac{1}{2}C_I\right\}\sin\ (2\pi f_0 t)+\left\{ky_0-\frac{1}{2}C_R\right\}\cos\ (2\pi f_0 t)=0 \tag{8}$$

The lift coefficient of the same phase with the response velocity, C_l, contributes to the damping of the system. The term which includes C_l is related with the aerodynamic damping. Here, considering the damping term in Eq. (8), the damping balance of the system is

$$d=\left\{2\pi f_0 y_0 c-\frac{1}{2}C_I\right\} \tag{9}$$

where the first term indicates the structural damping and the second term is referred to the aerodynamic damping. If the balance, *d,* becomes negative, the system tends toward oscillatory stability and the vibration of downstream cylinder becomes large since the negative damping effects on the response of the structure. And if the damping balance, *d,* goes to zero, the vibration becomes stabilized. Since the structural damping coefficient, *c*, is always positive, instability will occur only if

$$\left\{2\pi f_0 y_0 c-\frac{1}{2}C_I\right\}\le 0 \tag{10}$$

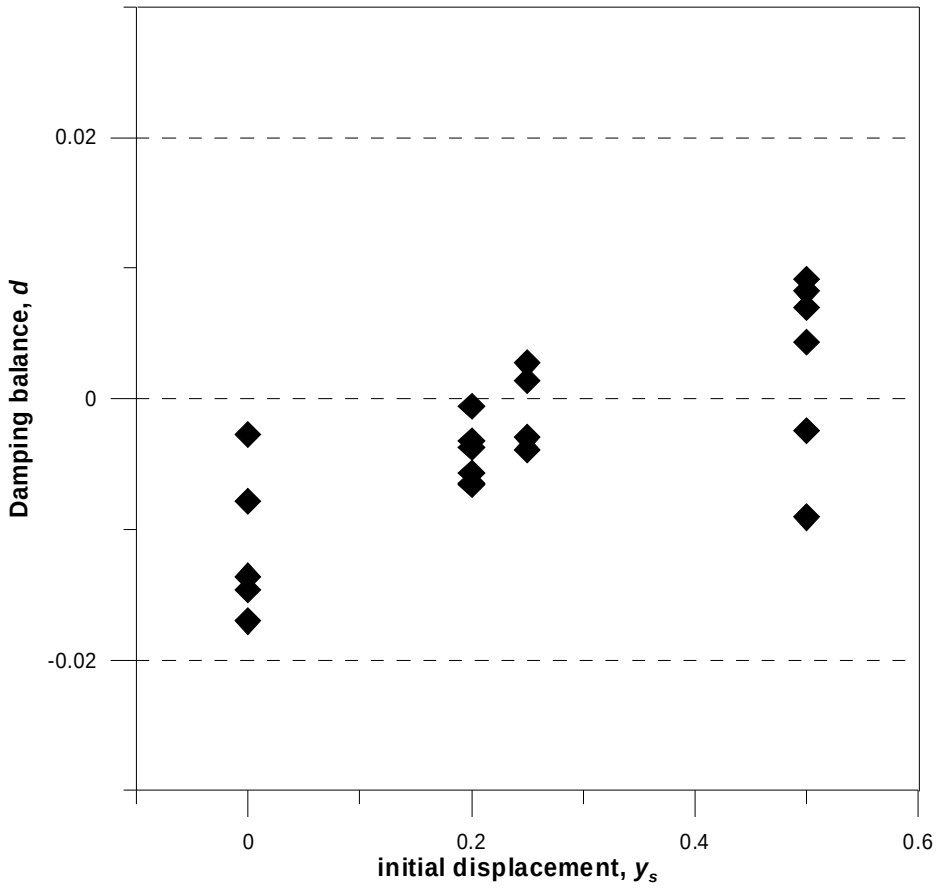

Fig.2. Damping balance, *d* with initial displacement, y_s= 0, 0.2, 0.25 and 0.5.

Fig. 2 shows the balances of damping in cases of the initial displacement, y_s = 0, 0.2, 0.25 and 0.5. Each damping balance is calculated with the peak amplitude of the response displacement in each case. Fig. 3 shows the non-dimensional responses of displacement. In case of y_s = 0, the damping balance, *d* is in negative so that the amplitude of the response displacement became larger as shown in Fig.3 (a). The amplitude of vibration in case of y_s = 0.5 was decreasing at the early time since the positive damping effects the vibration smaller. However, it also becomes stabilized as passing time. Since the damping balance, *d* becomes zero in cases of y_s = 0.2, 0.25 and 0.5, the amplitudes of vibration become stabilized as shown in Fig.3 (b), (c) and (d). To explain the relationship between the aerodynamic damping and oscillatory stabilization, the pressure distribution on the surface of downstream cylinder is verified in cases of y_s = 0.25 and 0.5. Also, the vorticity distributions are checked simultaneously.

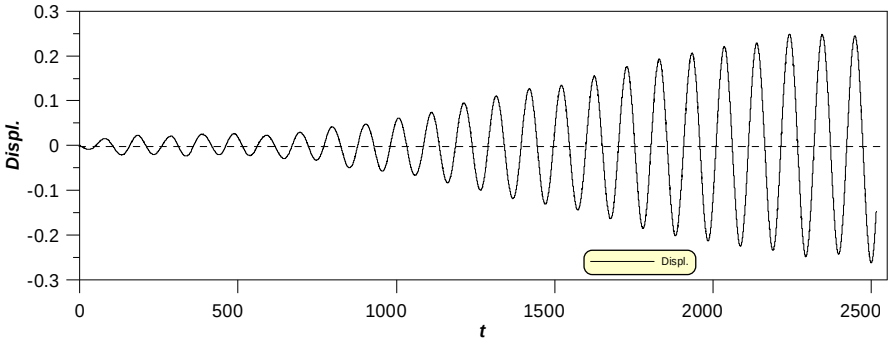

(a) Time history of the response displacement in case of y_s =0 at *U*=6.6m/s

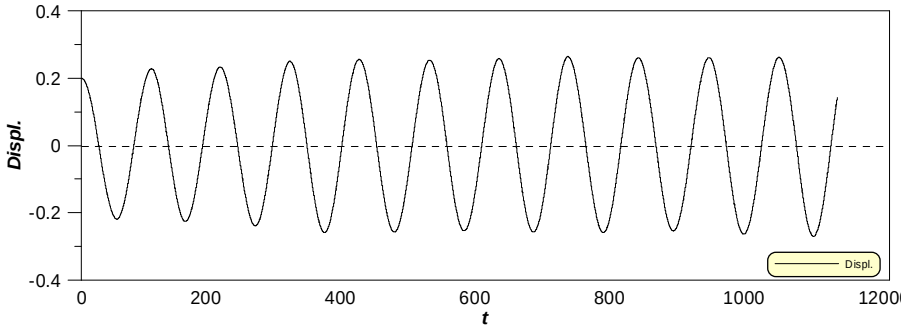

(b) Time history of the response displacement in case of y_s =0.2 at *U* =6.6m/s

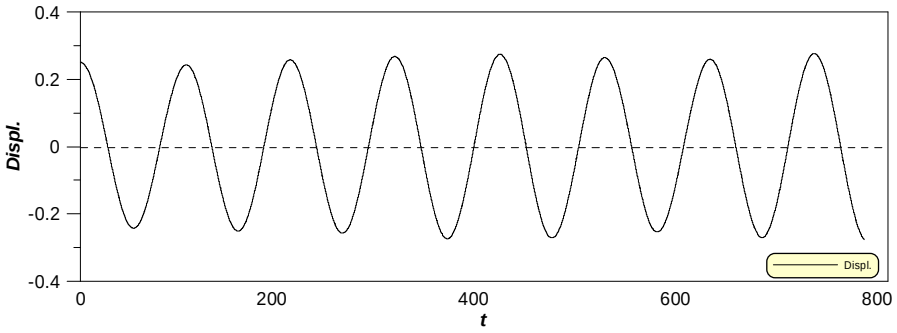

(c) Time history of the response displacement in case of y_s =0.25 at *U* =6.6m/s

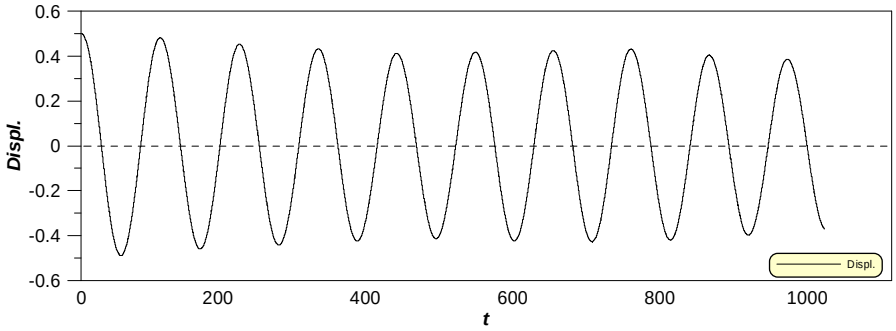

(d) Time history of the response displacement in case of y_s =0.5 at *U* =6.6m/s

Fig.3 The response displacements of downstream cylinder

3. AERODYNAMIC DAMPING EFFECT

3.1 The Positive Aerodynamic Damping Effect

When the lift coefficient of the same phase with response of velocity, C_I, is in negative, the positive aerodynamic damping effects on the system. In this case, the aerodynamic damping causes that the amplitude of the response displacement decreases. The value of *d* is in positive, which means

$$\left\{2\pi f_0 y_0 c - \frac{1}{2} C_I\right\} > 0 \tag{11}$$

In the range between dimensionless time *t*=753 and *t*=969 in case of y_s=0.5 at *U* =6.6m/s, the response amplitude of displacement decreases gradually as shown in Fig.3 (d).

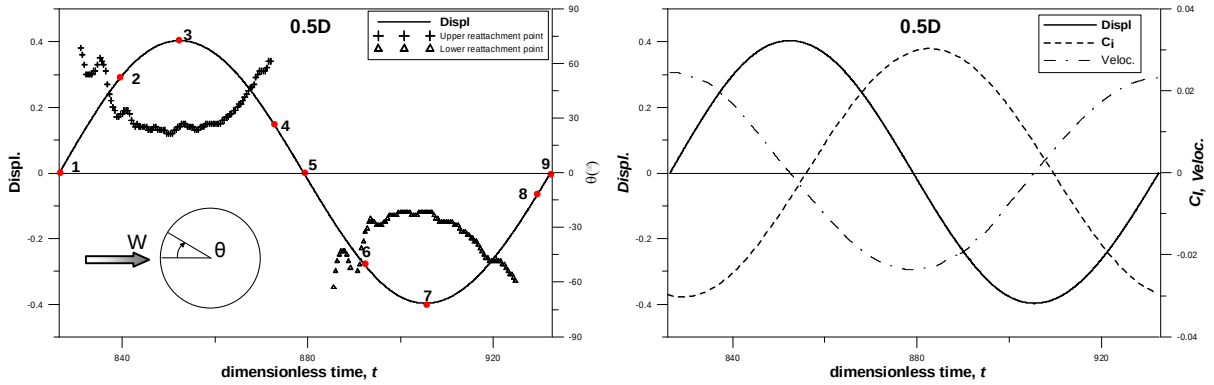

(a) Response displacement and reattachment points (b) Response displacement, velocity and C_I

Fig.4 Relationships between the responses in case of y_s = 0.5

To verify the aerodynamic positive damping effect, one period which has the decreasing part between dimensionless time *t*= 753 and *t*= 969 of the time history of displacement and that of the response velocity are considered with the reattachment points in Fig.4 (a). Fig.4 (b) represents the relationship between the response displacement, velocity and C_I. Where the response displacement had a positive peak which is at the point 3 in Fig.4, the value of velocity and C_I were almost zero. On the other hand, where the response displacement was zero at the point 5, the velocity had a negative peak and C_I had a positive peak value. The phase of the response displacement had different phase with the response velocity and C_I in half-phase difference as shown in Fig. 4 (b). The phase of the response velocity has the same phase with C_I but their signs were opposite.

To understand the positive aerodynamic damping effect, the vorticity distribution and the pressure distribution on the downstream-cylinder surface as shown in Fig.5 are investigated on each point represented in Fig.4 (a). At the point 1 and the point 9, where the response displacement was zero, the value of response velocity had positive maximum value represented as +V and the magnitude of the surface pressure was small. At the point 3 and the point 7, where the magnitude of response displacement had maximum, the value of response velocity was zero and the positive pressure occurred on the reattachment point represented as R in Fig.5.

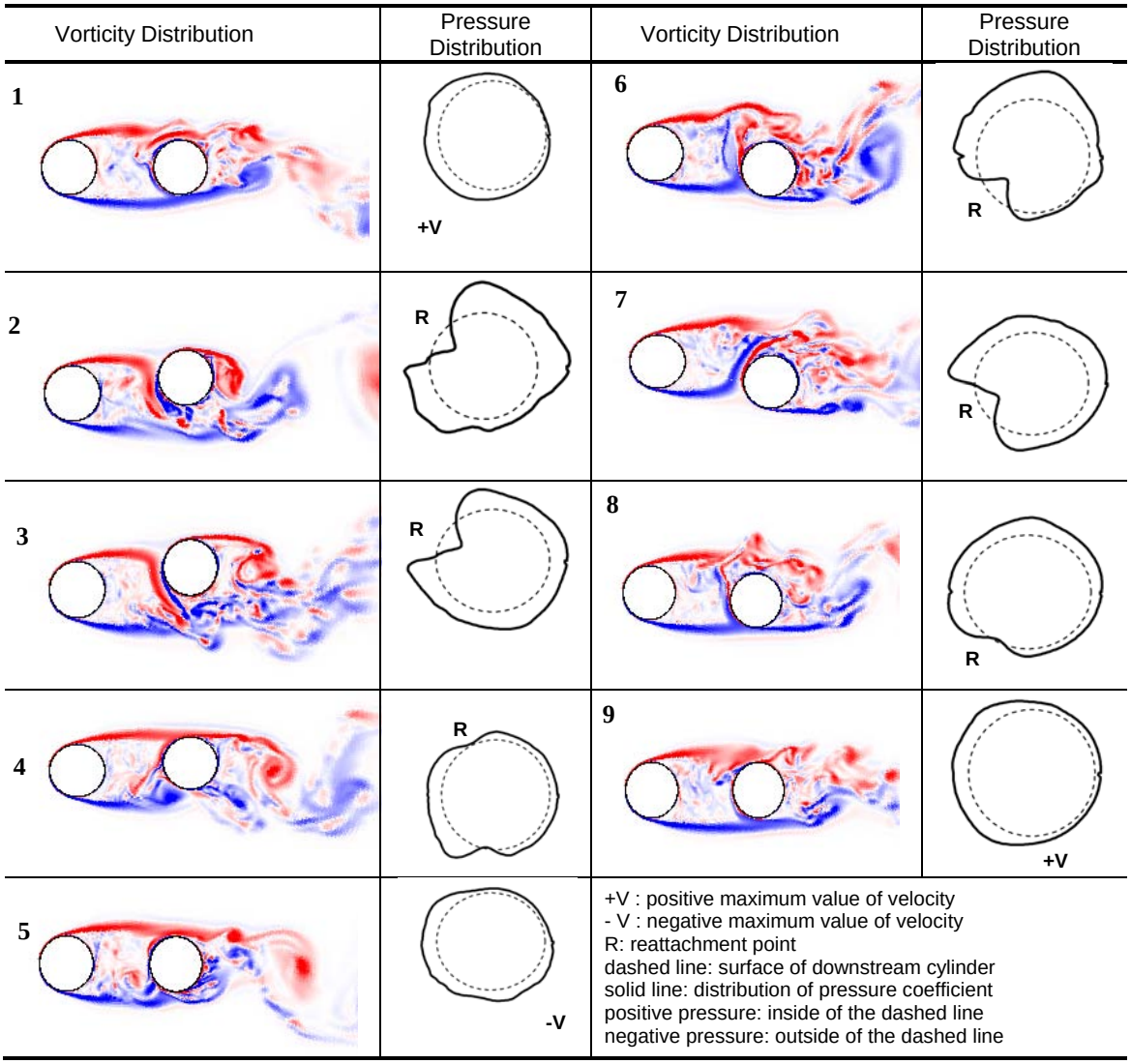

Fig.5 Relationship between the vorticity distribution and pressure distribution in case of $y_s = 0.5$

The non-dimensional pressure distribution on the downstream-cylinder surface is decomposed to understand each component's effect on the behavior of the downstream cylinder. The non-dimensional pressure on the cylinder surface is expressed as $p(\theta,t)$, where θ is the position on the cylinder surface (angle). By Fourier transform, the pressure which is the function of time became the function of the non-dimensional frequency. It means

$$p(\theta,t) \Rightarrow p(\theta, f) \tag{12}$$

where f is the non-dimensional frequency. The low-pass filtered non-dimensional pressure is represented as

$$p_{f \le f_0}(\theta, f) = \begin{cases} p(\theta, f) & (f \le f_0) \\ 0 & (f < f_0) \end{cases} \tag{13}$$

where f_0 is the non-dimensional natural frequency of the downstream cylinder. By Inverse Fourier transform,

$$p_{f \le f_0}(\theta,t) \quad \Leftarrow \quad p_{f \le f_0}(\theta, f) \tag{14}$$

The non-dimensional pressure having a single frequency of the natural frequency is expressed as $p(\theta, f_0)$. And it was decomposed into the component in same phase with the displacement of the downstream cylinder and that in same phase with the velocity of the cylinder. Namely,

$$p(\theta, f_0) \quad = \quad p^{displ.}(\theta, f_0) + p^{velo.}(\theta, f_0) \tag{15}$$

By Inverse Fourier transform for each component, the filtered non-dimensional pressure of each component is obtained as

$$\begin{cases} p_{f_0}^{displ.}(\theta,t) & \leftarrow & p_{f_0}^{displ.}(\theta, f_0) \\ p_{f_0}^{velo.}(\theta,t) & \leftarrow & p_{f_0}^{velo.}(\theta, f_0) \end{cases} \tag{16}$$

Since the aerodynamic damping is related with the response velocity, the pressure distribution only in case of $p_{f_0}^{velo.}(\theta,t)$ is investigated in Fig.6. Blue arrows indicate the direction of the downstream-cylinder movement (See Fig.5 and Fig.4 (a)). Red dashed arrows show the direction of the lift determined by the pressure component in phase with the velocity of the downstream cylinder due to the aerodynamic damping in Fig.6. For

example, since the upper part of downstream cylinder had positive pressures and the lower part had negative pressures at the point 1, the downstream cylinder tended to move to the downward direction. The direction of the cylinder movement (blue arrow) is opposite with that of the red arrow. The response amplitudes between dimensionless time *t*= 753 and *t*= 969 as shown in Fig.3 (d) are suppressed because of this positive aerodynamic damping effect.

No.	Direction of downstream cylinder movement	$p_{f_0}^{velo.}(\theta,t)$	No.	Direction of downstream cylinder movement	$p_{f_0}^{velo.}(\theta,t)$
1	↑	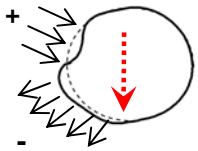	6	↓	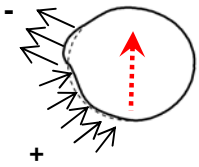
2	↑	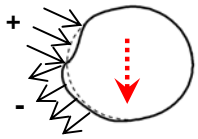	7		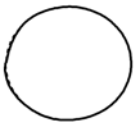
3		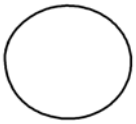	8	↑	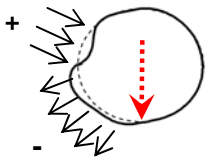
4	↓	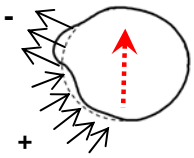	9	↑	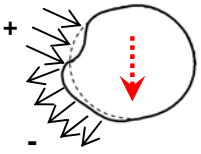
5	↓	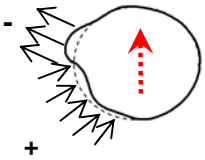	- Red dashed arrows represent the direction of the cylinder due to aerodynamic damping effect. - Black arrows on the surface pressure represent the sign of pressure : + : positive pressure, - : negative pressure		

Fig.6 Pressure distribution on downstream cylinder in case of $p_{f_0}^{velo.}(\theta,t)$. (y_s = 0. 5)

3.2 The Negative Aerodynamic Damping Effect

When the lift coefficient of the same phase with the response velocity C_l, is positive, three conditions are occurred depending on the balance of damping. If the aerodynamic damping term is smaller than the structural damping term, the whole of damping becomes positive and the amplitudes of response displacement decrease. If the aerodynamic damping term is same as the structural damping term, the amplitudes of response displacement become stabilized. If the aerodynamic damping term is larger than the structural damping term, the negative damping effects on the whole system and also the damping balance becomes negative. In this case, the amplitude of response displacement becomes larger.

The balance d is in negative when the aerodynamic damping is larger than the structural damping, which means

$$\left\{2\pi f_0 y_0 c - \frac{1}{2} C_I\right\} < 0 \tag{17}$$

One period which has the increasing part between dimensionless time t= 597 and t= 701 of the time history of response displacement in case of y_S= 0.25 is considered with the reattachment points in Fig.7 (a). Fig.7 (b) represents the relationship between the response displacement, velocity and C_l. Where the response displacement had a positive peak which is at the point 3 in Fig.7 (a), the value of velocity and C_l were almost zero. On the other hand, where the response displacement was zero at the point 5, both of the velocity and C_l had a negative peak value. The phase of the response displacement had different phase with the response velocity and C_l in the half-phase difference as shown in Fig. 7 (b). The phase of the response velocity has the same phase with C_l and their signs were same.

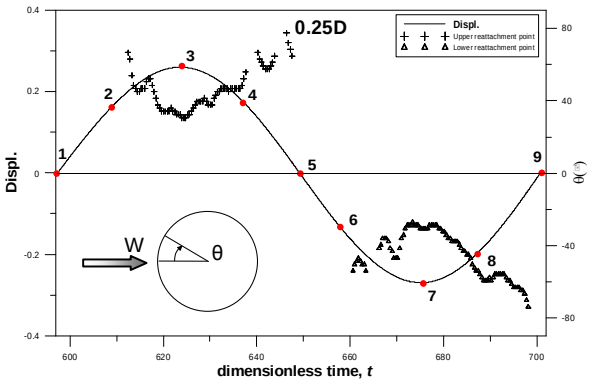

(a) Response displacement and reattachment points

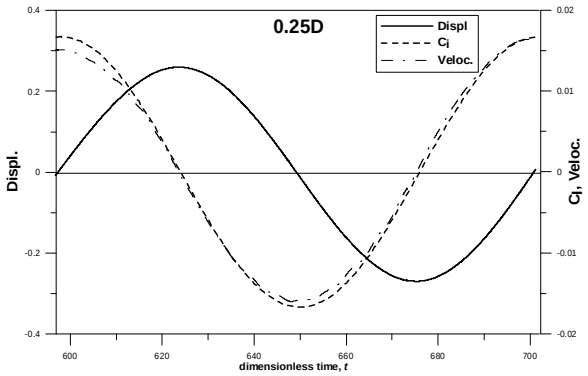

(b) Response displacement, velocity and C_l

Fig.7 Relationships between the responses in case of y_s = 0.25

To understand the negative aerodynamic damping effect, the vorticity distribution and the pressure distribution on the downstream-cylinder surface as shown in Fig.8 are investigated on each point represented in Fig.7 (a). In the point 1 and point 9, where the response displacement was zero, the value of response velocity had positive maximum value represented as +V and the magnitude of the surface pressure was small. In the point 3 and the point 7, where the magnitude of response displacement had maximum, the value of response velocity was zero and the positive pressure occurred on the reattachment point represented as R in Fig.8.

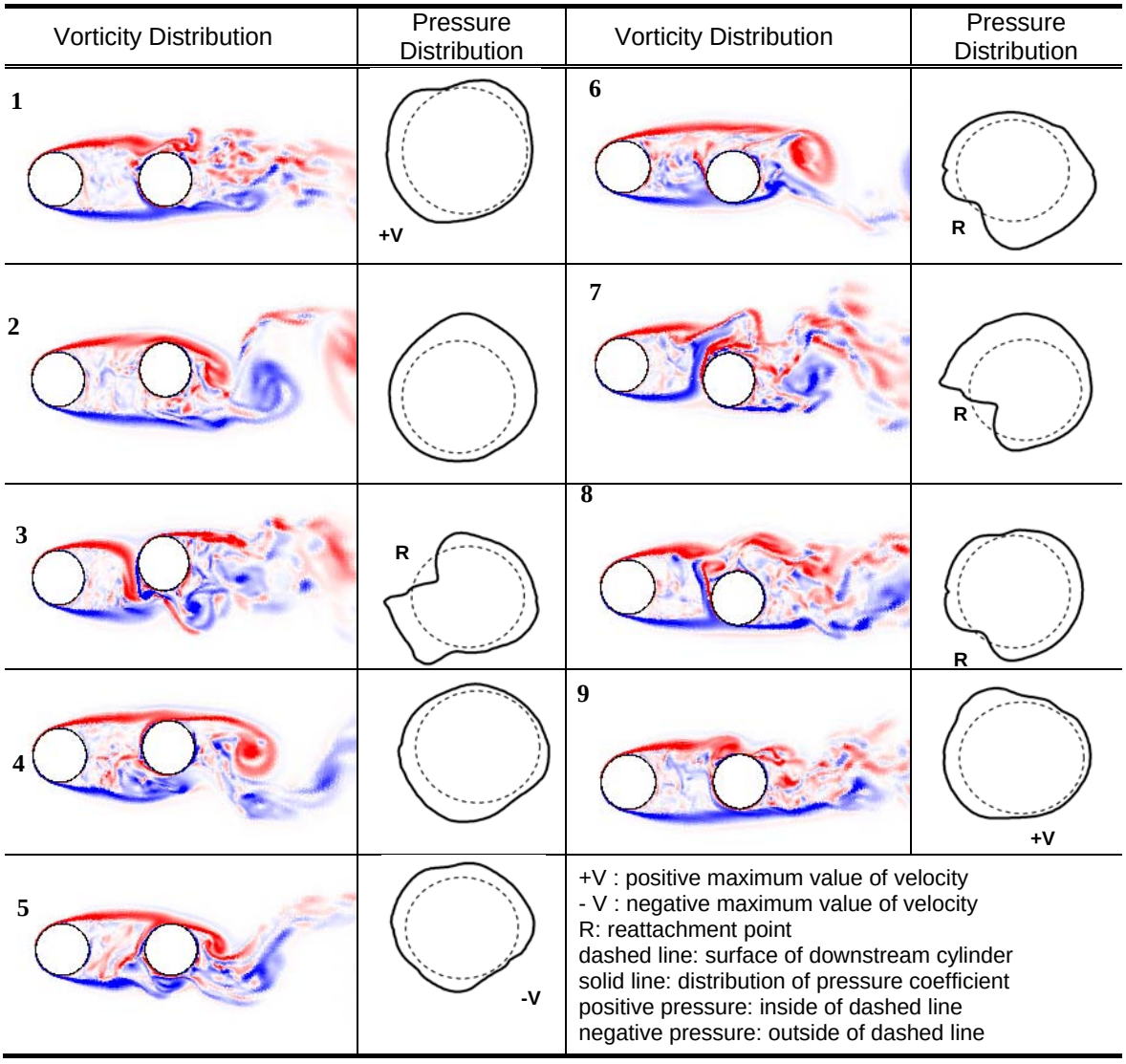

Fig.8 Relationship between the vorticity distribution and pressure distribution in case of y_s = 0.25

No.	Direction of downstream cylinder movement	$p_{f_0}^{velo.}(\theta,t)$	No.	Direction of downstream cylinder movement	$p_{f_0}^{velo.}(\theta,t)$
1		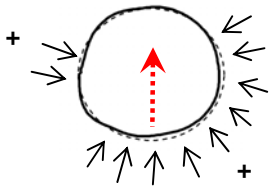	6		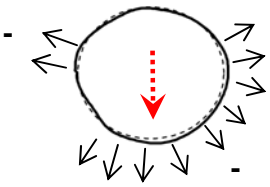
2		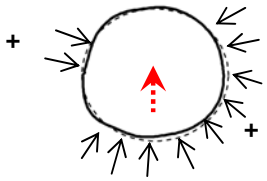	7		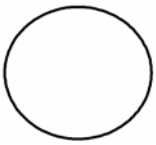
3		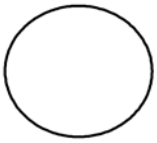	8		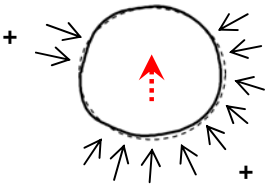
4		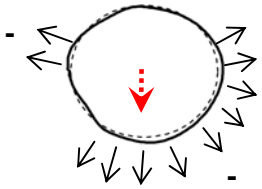	9		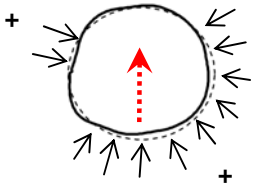
5		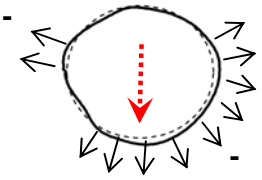	- Red dashed arrows represent the direction of the cylinder due to aerodynamic damping effect. - Black arrows on the surface pressure represent the sign of pressure : + : positive pressure, - : negative pressure		

Fig.9 Pressure distribution on downstream cylinder in case of $p_{f_0}^{velo.}(\theta,t)$. (y_s = 0. 25)

Since the aerodynamic damping is related with the response velocity, the pressure distribution only in case of $p_{f_0}^{velo.}(\theta,t)$ is investigated in case of y_s =0.25 in Fig.9. Blue arrows indicate the moving direction of the downstream-cylinder movement (See Fig.9 and Fig.7 (a)). Red dashed arrows show the direction of the lift determined by the pressure component in phase with the velocity of the downstream cylinder due to the aerodynamic

damping in Fig.9. For example, since the lower part of the cylinder surface had positive pressures at the point 1, the downstream cylinder tended to lift the upward direction. Blue arrows represented the direction of the downstream-cylinder movement have the same direction with red arrows. The response amplitudes between dimensionless time t= 597 and t= 701 as shown in Fig.3 (c) become larger because of this negative aerodynamic damping effect.

When the aerodynamic damping term and the structural damping term have the same value and the opposite sign each other as expressed in Eq. (18), the amplitudes of response displacement become stabilized. The value of *d* is zero, which means

$$\left\{ 2\pi f_0 y_0 c - \frac{1}{2} C_I \right\} = 0 \tag{18}$$

These balanced cases were also investigated and they had same trends to the values of $p_{f_0}^{velo.}(\theta,t)$ and C_l with those that had the negative aerodynamic damping effect.

4. CONCLUSIONS

To clarify the mechanism of the wake galloping, the aerodynamic damping effect is investigated. The balance of structural damping and aerodynamic damping is important factor to divide to three patterns of the vibration on downstream cylinder. In the first pattern, when the aerodynamic damping is smaller than the structural damping, the balance becomes in positive. The positive aerodynamic damping helps suppressing the amplitudes of vibration. In the second one, when the aerodynamic damping is the same with the structural damping, the balance becomes zero and the amplitudes of vibration become stabilized. In the most cases of this research, the amplitudes of response displacement on downstream cylinder were stabilized and the vibrations were not suppressed and became the same shape as free vibration because of this balanced damping. In the third pattern, when the aerodynamic damping is larger than the structural damping, the balance becomes in negative and the amplitudes of vibration in downstream cylinder become larger. The negative aerodynamic damping makes the downstream cylinder vibrate continuously and even more large.

The aerodynamic damping effect is explained with the component in phase with the velocity of non-dimensional pressure having a single frequency equal to the natural frequency, $p_{f_0}^{velo.}(\theta,t)$. In case of positive aerodynamic damping, the direction of the lift determined by $p_{f_0}^{velo.}(\theta,t)$ was the opposite direction with the direction of the downstream-cylinder movement. Therefore, the response amplitudes of downstream cylinder became smaller. In case of the balanced damping, the direction of the lift determined by $p_{f_0}^{velo.}(\theta,t)$ was the opposite direction with the direction of the downstream-cylinder movement. Therefore, the response amplitudes of downstream cylinder became stabi-

lized because the structural damping and aerodynamic damping were balanced. In case of negative aerodynamic damping, the direction of the lift determined by $p_{f_0}^{velo.}(\theta,t)$ acted the same direction with the direction of the downstream-cylinder movement. Therefore, the response amplitudes of downstream cylinder became larger.

REFERENCES

Kim, H.Y., Kitagawa, T. (2011), "Numerical investigation of wake galloping around two circular cylinders"*, 13th International Conference of Wind Engineering, ICWE13*.

Kim, H.Y., Liu, Kitagawa, T., Dragomirescu, E. (2008), "Flow-force relationship for two staggered circular cylinders with low angle of incidence"*, Journal of Structural Engineering, JSCE,* 54A, 411-419.

Kitagawa, T. and Ohta, H. (2008), "Numerical investigation on flow around circular cylinders in tandem arrangement at a subcritical Reynolds number", *Journal of Fluids and Structures*, Vol. 24, pp. 680-699.

Igarashi, T. (1984), "Characteristics of the flow around two circular cylinders arranged in tandem 2nd report ; unique phenomenon at small spacing", *Bulletin of JSME*, B27, 2380-2387.

Gu, Z. & Sun, T. (1984), "On interference between two circular cylinders in staggered arrangement at high subcritical Reynolds numbers", *Journal of Wind Engineering and Industrial Aerodynamics*, 80, 287-309.

Sun, T. F., Gu, Z. F., He, D. X. & Zhang, L. L. (1992), "Fluctuating pressure on two circular cylinders at high Reynolds numbers", *Journal of Wind Engineering and Industrial Aerodynamics*, 41-44, 577-588.

Zhang, H. & Melbourne, W. H. (1992), "Interference between two circular cylinders in tandem in turbulent flow", *Journal of Wind Engineering and Industrial Aerodynamics*, 41-44, 589-600.

Mittal, S. & Kumar, V. (2001), "Flow-induced oscillations of two cylinders in tandem and staggered arrangements", *Journal of Fluids and Structures*, 15, 717-736.

Bokaian, A. & Geoola, F. (1984), "Wake-induced galloping of two interfering circular cylinders", *Journal of Fluid Mechanics*, 146, 383-415.

Bearman, P. W. & Wadcock, A. J. (1973), "The interaction between a pair of circular cylinders normal to a stream", *Journal of Fluid Mechanics*, 61, 499-511.

King, R. & Johns, D. J. (1976), "Wake interaction experiments with two flexible circular cylinders in flowing water", *Journal of Sound and Vibration*, 45, 259-283.

Rupert G. Williams, Wimal Suaris (2006), "An analytical approach to wake interference effects on circular cylindrical structures", *Journal of Sound and Vibration s*, 295, 266-281.

Williamson, C. H. K.: Evolution of a single wake behind a pair of bluff bodies, *Journal of Fluid Mechanics*, 159, 1-18, 1985.